Synergistic Enhancement of Ternary Poly(3,4-ethylenedioxythiophene)/Graphene Oxide/Manganese Oxide Composite as a Symmetrical Electrode for Supercapacitors

Nur Hawa Nabilah Azman [1], Hong Ngee Lim [1,2] (iD), Md Shuhazlly Mamat [3] and Yusran Sulaiman [1,4,* (iD)]

[1] Department of Chemistry, Faculty of Science, Universiti Putra Malaysia,
    Serdang 43400 UPM, Selangor, Malaysia; hawa_nabilah@yahoo.com (N.H.N.A.);
    hongngee@upm.edu.my (H.N.L.)
[2] Functional Devices Laboratory, Institute of Advanced Technology, Universiti Putra Malaysia,
    Serdang 43400 UPM, Selangor, Malaysia
[3] Department of Physics, Faculty of Science, Universiti Putra Malaysia,
    Serdang 43400 UPM, Selangor, Malaysia; shuhazlly@upm.edu.my
[4] Materials Synthesis and Characterization Laboratory, Institute of Advanced Technology,
    Universiti Putra Malaysia, Serdang 43400 UPM, Selangor, Malaysia
*   Correspondence: yusran@upm.edu.my; Tel.: +60-3-8946-6779

Abstract: A novel facile preparation of poly(3,4-ethylenedioxythiophene)/graphene oxide/manganese oxide ($PEDOT/GO/MnO_2$) ternary composite as an electrode material for a supercapacitor was evaluated. The ternary composite was sandwiched together and separated by filter paper soaked in 1 M KCl in order to investigate the supercapacitive properties. The ternary composite exhibits a higher specific capacitance (239.4 F/g) compared to PEDOT/GO (73.3 F/g) at 25 mV/s. The incorporation of MnO_2 which act as a spacer in the PEDOT/GO helps to improve the supercapacitive performance by maximizing the utilization of electrode materials by the electrolyte ions. The $PEDOT/GO/MnO_2$ ternary composite displays a specific energy and specific power of 7.9 Wh/kg and 489.0 W/kg, respectively. The cycling stability test revealed that the ternary composite is able to achieve 95% capacitance retention even after 1000 cycles due to the synergistic effect between the PEDOT, GO, and MnO_2 that helps to enhance the performance of the ternary composite for supercapacitor application.

Keywords: supercapacitor; poly(3,4-ethylenedioxythiophene); graphene oxide; manganese oxide

1. Introduction

Metal oxides such as ruthenium oxide (RuO_2), manganese oxide (MnO_2), and iron oxide (Fe_2O_3) are considered as ideal electrode materials for pseudocapacitors as metal oxides offer superior specific energy and electrochemical stability in comparison to carbon-based and polymer materials [1,2]. RuO_2 is one of the most promising metal oxides to be used as an electrode material due to its good pseudo-capacitive performance, wide-range potential window, and various oxidation states (Ru^{2+}, Ru^{3+}, and Ru^{4+}) among other metal oxides [3,4].

Regardless of its enormous pseudocapacitive performance, RuO_2 is very expensive and toxic to the environment. Thus, many researchers are exploring for other alternative metal oxides, in which MnO_2 becomes a substitute for RuO_2 to reduce the production cost and prevent environmental problems.

In comparison to RuO_2, manganese oxide is low-cost and harmless to the environment. Moreover, manganese oxide also offers high capacitance and possesses similar electrochemical behavior to RuO_2 [1]. Nevertheless, the limitations of MnO_2 are poor electrical conductivity, low life cycle, and poor mechanical stability where these properties are important for supercapacitors. A polythiophene derivative such as poly(3,4-ethylenedioxythiophene) (PEDOT) is a suitable candidate to be used as an electrode material as PEDOT possesses high electrical conductivity and is environmentally friendly [5]. In addition, graphene oxide (GO) has become the main material for supercapacitor application due to its high mechanical strength and high surface area. GO is hydrophilic in nature as a result of the presence of polar groups such as hydroxyl, epoxide, and carboxyl that make the GO easily disperse in water.

Many researchers have studied composites consisting of carbon-based materials and conducting polymer as electrode materials for supercapacitors. Cha, et al. [6] developed a composite of polydopamine-graphene oxide/poly(3,4-ethylenedioxythiophene) (PDA–GO/PEDOT) and achieved a specific capacitance of 126 F/g with capacitance retention of 75% even after 1000 cycles. Besides that, Soojeong, et al. [7] studied the supercapacitive performance of PEDOT/graphene composite prepared via electrodeposition. The PEDOT/graphene composite possesses a specific capacitance of 154 F/g which is superior to that of PEDOT (only 42.6 F/g). Recently, the rapid development of worldwide research on the performance of supercapacitors has upgraded the study of electrode material for supercapacitors to another level whereby ternary composites consisting of carbon-based material, conducting polymer, and metal oxide are renowned in further enhancing the supercapacitive performance of the composites. Graphite/PEDOT/MnO_2 ternary composite has been synthesized and exhibited a high specific capacitance (195.7 F/g) with specific energy and specific power of 31.4 Wh/kg and 90 W/kg, respectively. In addition, the composite was able to retain 81.1% of its original specific capacitance after 2000 cycles [8]. A new poly(3,4-ethylenedioxythiophene): poly(styrenesulfonate)/manganese oxide/reduced graphene oxide (PEDOT:PSS/MnO_2/rGO) showed a potential as an electrode material for supercapacitors and was able to exhibit a specific capacitance of 169.1 F/g with 66.2% capacitance retention after 2000 cycles [9]

Herein, we report a one-step electrodeposition of PEDOT/GO/MnO_2 ternary composite as an electrode material. The ternary composite was electrodeposited at 1.2 V for 10 min. The supercapacitive performance of the PEDOT/GO/MnO_2 was investigated and compared with the binary composite and the effect of varying the loading amount of manganese salt precursor on the performance of the supercapacitor was studied.

## 2. Results

2.1. Morphological and Structural Analysis

Figure 1 shows field emission scanning electron microscopy (FESEM) images of PEDOT/GO/MnO_2 and PEDOT/GO. Figure 1a reveals the FESEM image of PEDOT/GO with typical crumpled and wrinkled paper-like sheet morphology. The crumpled and clear wrinkles that can be seen in the morphology of PEDOT/GO are a result of the repulsive force between the negative charge GO sheets [10] and the defects produced during the breaking up of the sp^2 hybridized graphene structure [11]. The combination of PEDOT and GO cause the surface of the prepared PEDOT/GO to become rougher and the wrinkled paper like-sheets of GO become more prominent [12]. The evidence of the incorporation of MnO_2 into the binary composite can be clearly seen from the presence of MnO_2 particles on the wrinkled paper-like sheets of PEDOT/GO (Figure 1b). In addition, the presence of MnO_2 (insert Figure 1b) can act as a spacer in order to prevent the agglomeration of GO sheets [13].

The structural analyses of GO, PEDOT, PEDOT/GO and PEDOT/GO/MnO_2 (Figure 2) were performed using Raman spectroscopy. The Raman spectra of GO (Figure 2a) displays distinctive peaks at 1600 and 1350 cm^{-1}, which are associated with G and D bands, respectively. The G band is attributed to sp^2 hybridized carbon atoms while the D band is related to sp^3 hybridized carbon atoms

and defects in the structure [10]. As for PEDOT/GO (Figure 2b), Raman bands at 1500 and 1430 cm^{-1} correspond to the asymmetric and symmetric C=C stretching whereas Raman bands at 1361, 1265, and 1108 cm^{-1} are attributed to C$_{\alpha}$-C$_{\alpha'}$, C$_{\beta}$-C$_{\beta'}$ stretch, and C-O-C respectively. The Raman bands at 985, 578, and 428 cm^{-1} are associated with the oxyethylene ring. D band is hardly distinguished in the Raman spectra of PEDOT/GO and also PEDOT/GO/MnO$_2$ (Figure 2c) as the D band is overlapped with the C-C bond in PEDOT. Nevertheless, an extra peak can be observed in the Raman spectra of PEDOT/GO and PEDOT/GO/MnO$_2$ at ~1600 cm^{-1} which originates from G band of GO. As shown in Figure 2c, all the Raman bands of PEDOT and GO are present in the Raman spectrum of PEDOT/GO/MnO$_2$, implying that PEDOT is successfully incorporated. The presence of MnO$_2$ in the PEDOT/GO/MnO$_2$ can be confirmed by the presence of Raman bands at 684 cm^{-1} [14]. Another peak of MnO$_2$ at 578 cm^{-1} [8] is also observable in the Raman spectrum of PEDOT/GO/MnO$_2$, however, this peak is overlapped with the oxoethylene ring of PEDOT. It was observed that this peak became more intense after incorporation of MnO$_2$ indicating successful incorporation of MnO$_2$ into the ternary composite.
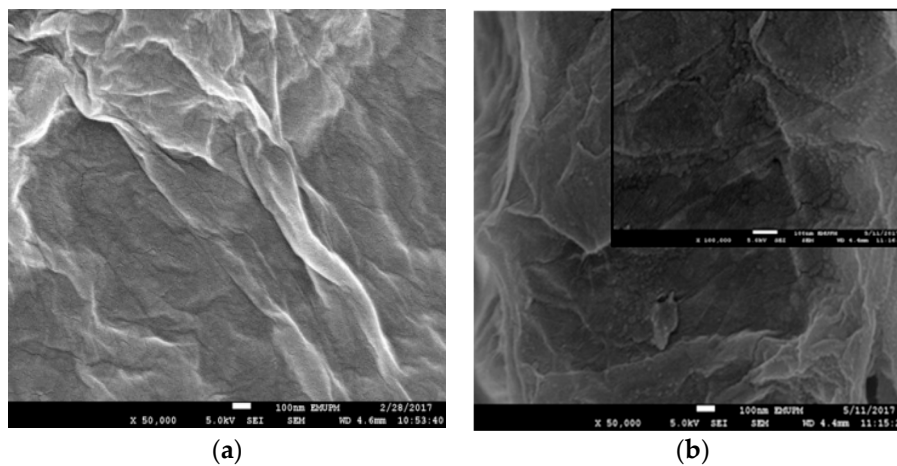

Figure 1. Field emission scanning electron microscopy (FESEM) images of (**a**) PEDOT/GO and (**b**) PEDOT/GO/MnO$_2$ (inset: high magnification of PEDOT/GO/MnO$_2$).
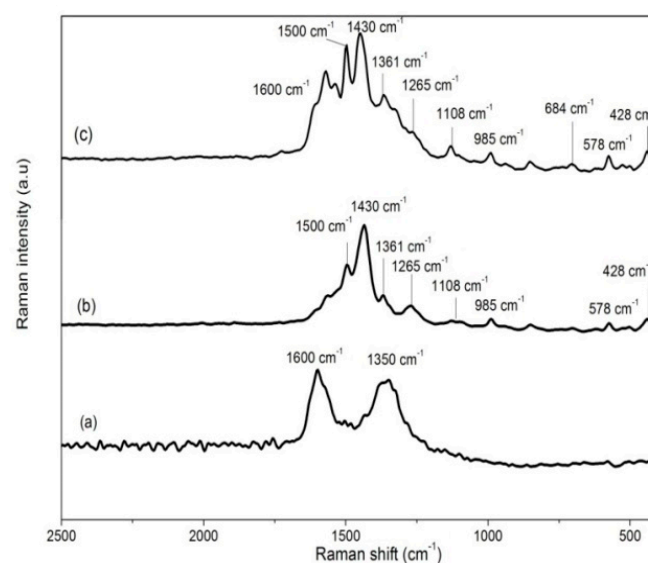

Figure 2. Raman spectra of (**a**) GO, (**b**) PEDOT/GO, and (**c**) PEDOT/GO/MnO$_2$.

The elemental analysis of PEDOT/GO/MnO$_2$ was further characterized by X-ray photoelectron spectrometry (XPS. As displayed in Figure 3a, the C 1s spectrum of PEDOT/GO/MnO$_2$ is deconvoluted into five distinct peaks. The main peak of the C 1s spectrum corresponds to the C-C/C=C at a binding energy of 284.6 eV. The binding energy at 285.8 eV is assigned to C-S which originates from PEDOT. The peak of C-O (epoxy and hydroxyl) which originates from GO can be observed at 286.7 eV and the peaks of C=O and O-C=O are illustrated at binding energies of 287.9 and 288.9 eV respectively. The incorporation of MnO$_2$ into the PEDOT/GO/MnO$_2$ ternary composite is proven from the XPS spectrum of Mn 2p (Figure 3b). The Mn 2p XPS spectrum displays two deconvoluted peaks which are Mn 2p$_{3/2}$ at a binding energy of 641.9 eV and Mn 2p$_{1/2}$ at 653.7 eV with energy separation of 11.8 eV which is attributed to Mn^{4+} in MnO$_2$ [15].
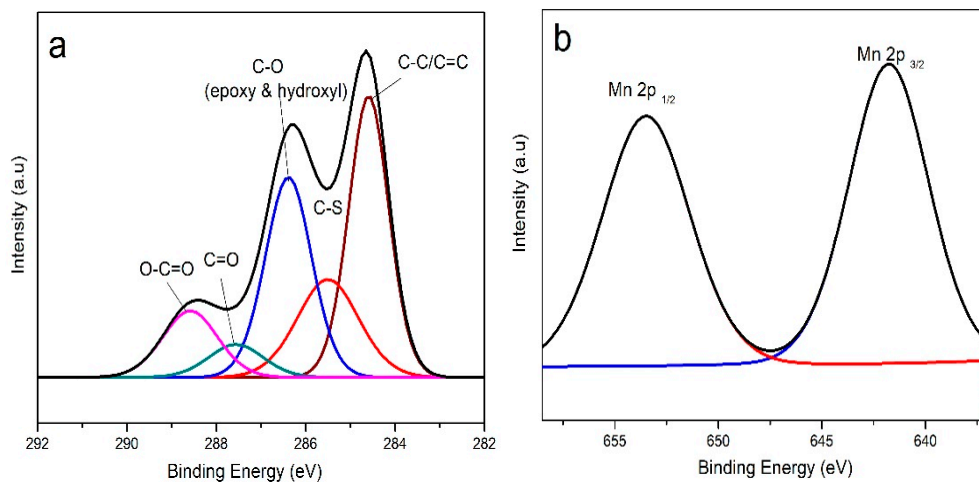
Figure 3. X-ray photoelectron spectrum (XPS) of PEDOT/GO/MnO$_2$, (**a**) C 1s and (**b**) Mn 2p.

Figure 4a reveals X-ray diffraction (XRD) peaks at 24° corresponding to the (020) diffraction plane of PEDOT/GO. After the addition of MnO$_2$ into PEDOT/GO (Figure 4b), there are three additional peaks at 28°, 38°, 43°, 56°, and 64° attributed to the (110), (101), (111), (211), and (020) diffraction planes of MnO$_2$ [16], indicating the successful incorporation of MnO$_2$ in the composite (JCPDS No. 24-0735).
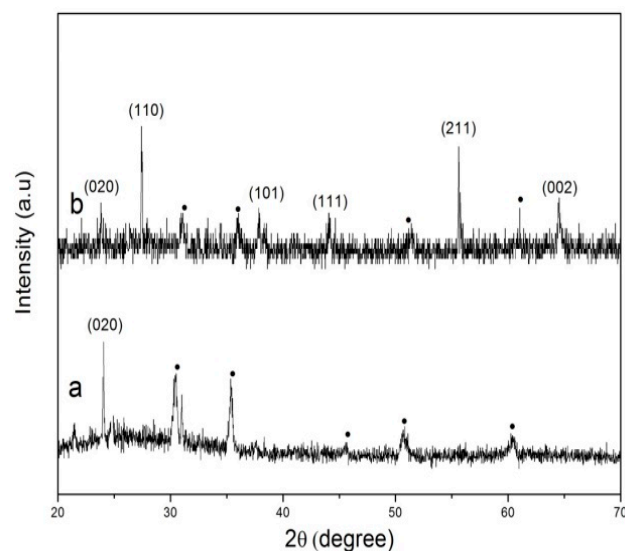
Figure 4. X-ray diffraction (XRD) pattern of (**a**) PEDOT/GO and (**b**) PEDOT/GO/MnO$_2$. Peaks labeled corresponding to the peaks of ITO substrate.

2.2. Electrochemical Measurements

　　The symmetric supercapacitor based PEDOT/GO/MnO$_2$ was expected to show good supercapacitive behavior. The effect of manganese oxide loading on the ternary PEDOT/GO/MnO$_2$ composite was evaluated via cyclic voltammetry at 25 mV/s to optimize the amount of manganese oxide to be incorporated with PEDOT/GO (Figure 5a). The specific capacitance exhibited by the ternary composite is displayed in Figure 5b. The cyclic voltammograms (CVs) of PEDOT/GO/MnO$_2$ at different concentrations show quasi-rectangular shape with redox peaks. At 0.025 M of the manganese precursor, the ternary composite exhibits low specific capacitance as a result of a too small amount of manganese precursor which only has a slight effect on the specific capacitance. As the amount of manganese precursor is increased to 0.05 M, a sharp increase of specific capacitance (239.4 F/g) with the largest enclosed CV area is observed. The specific capacitance is comparable to that of PEDOT/graphene/SnO$_2$ [17]. As the amount of manganese precursor is further increased, the cyclic voltammogram area of the PEDOT/GO/MnO$_2$ gradually decrease due to the high amount of MnO$_2$ that limits the charge storing ability of the ternary composite as MnO$_2$ suffers from low conductivity [18,19].
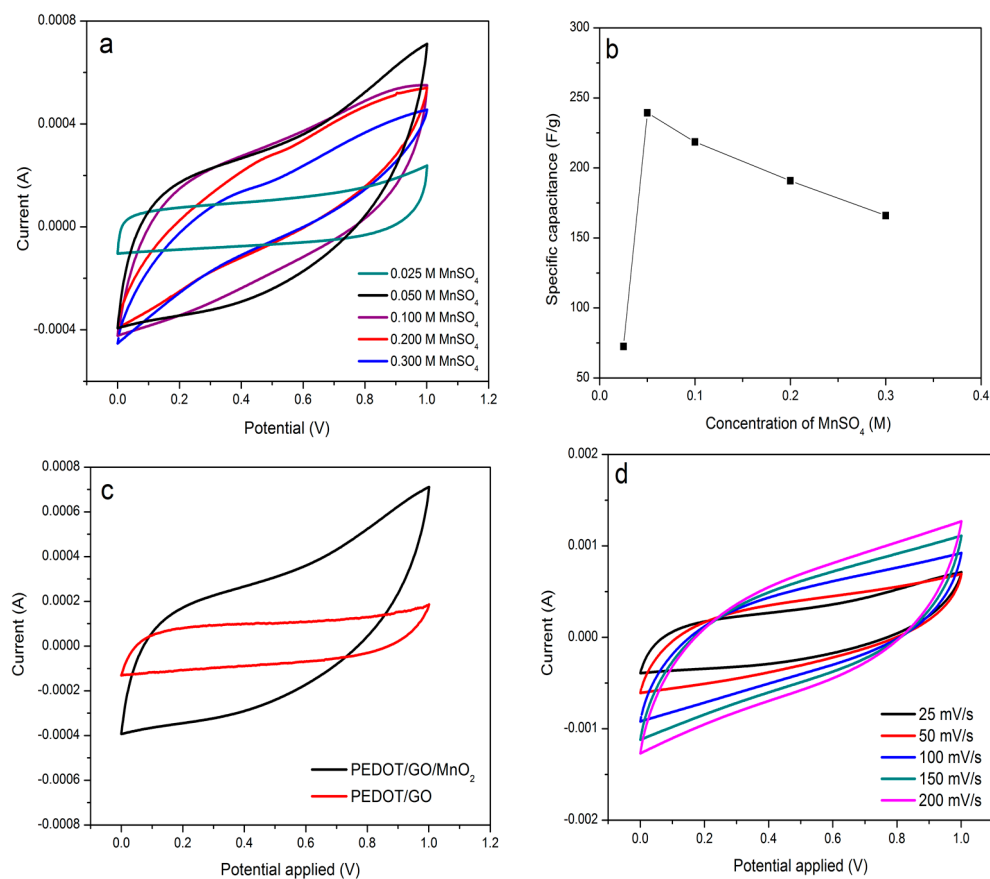

Figure 5. (**a**) Cyclic voltammograms (CVs) of PEDOT/GO/MnO$_2$ with different manganese loading, at 25 mV/s; (**b**) specific capacitance of PEDOT/GO/MnO$_2$ with different concentration of manganese, at 25 mV/s; (**c**) CVs of PEDOT/GO and PEDOT/GO/MnO$_2$, at 25 mV/s; (**d**) CVs of PEDOT/GO/MnO$_2$ at different scan rates.

　　The PEDOT/GO/MnO$_2$ with the highest specific capacitance was compared with PEDOT/GO as shown in Figure 5c. As can be seen, the introduction of MnO$_2$ into the PEDOT/GO composite enhances the supercapacitive performance due to the synergistic effects of the combined materials and the properties of MnO$_2$ which is known for its high specific capacitance [20]. In addition, MnO$_2$

which acts as spacer prevents restacking of the GO layers [21] due to the large Van der Waals interaction that limits the effective surface for electrochemical reaction. Therefore, the addition of MnO_2 helps to increase the surface area of the ternary composite and maximize the utilization of electrode materials by the electrolyte ions [22]. As shown in Figure 5d, the shape of the cyclic voltammogram of PEDOT/GO/MnO_2 at different scan rates as shown remains the same even at high scan rates implying excellent supercapacitive performance and charge storing behavior.

Galvanostatic charge-discharge (GCD) was carried out in order to further study the supercapacitive behavior of the ternary composite by varying the current densities from 1 A/g to 5 A/g. As can be seen in Figure 6a, the GCD curves of PEDOT/GO/MnO_2 at all current densities show an asymmetrical triangle shape implying the presence of pseudocapacitance behavior of the materials [23]. As expected the process of charging/discharging of PEDOT/GO/MnO_2 at the lowest current density is the longest. This phenomenon is due to the adequate insertion and release of electrolyte ions throughout the process of charging/discharging [24]. At high current density, the process of charging/discharging decreases which is attributed to the inadequate interaction of electrolyte ions between the electrode and electrolyte [25,26].
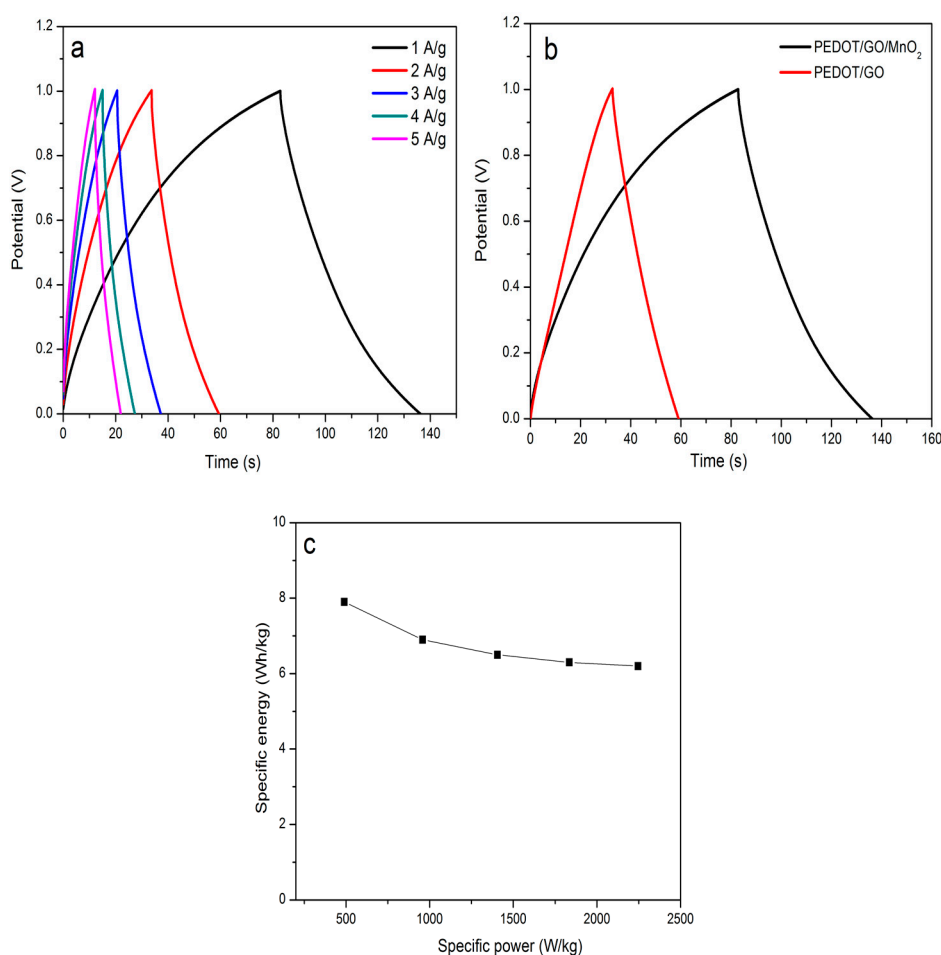

Figure 6. Galvanostatic charge-discharge (GCD) of (**a**) PEDOT/GO/MnO_2 at different current densities, (**b**) PEDOT/GO/MnO_2 and PEDOT/GO, and (**c**) Ragone plot of PEDOT/GO/MnO_2.

The GCD curves of PEDOT/GO/MnO_2 and PEDOT/GO are compared at 1 A/g as depicted in Figure 6b. PEDOT/GO/MnO_2 displays longer discharging time indicating a better charging/ discharging performance compared to PEDOT/GO. The better performance of PEDOT/GO/MnO_2 indicates that the incorporation of MnO_2 helps to improve the supercapacitive performance of the

ternary composite. The Ragone plot (Figure 6c) demonstrates that the maximum specific energy achieved by PEDOT/GO/MnO$_2$ is 7.9 Wh/kg with a specific power of 489.0 W/kg at the lowest current density (1 A/g). The specific energy and power obtained at the highest current density (5 A/g) are 6.2 Wh/kg and 2246.6 W/kg, respectively.

In order to study the conductivity performances of the PEDOT/GO/MnO$_2$, electrochemical impedance spectroscopy (EIS) was performed. Figure 7 presents the Nyquist plot of PEDOT/GO/MnO$_2$ and PEDOT/GO. The diameter of the semicircle provides the information on the resistance charge transfer (R_{ct}) of the materials at the electrode/electrolyte interface. A large semicircle demonstrates larger R_{ct} which is not favorable for a supercapacitor. As seen in the inset of Figure 7a, the high frequency region of the Nyquist plot of PEDOT/GO/MnO$_2$ shows a semicircle with smaller diameter (6.2 Ω) after incorporation of MnO$_2$ compared to the binary PEDOT/GO (20.1 Ω) composite indicating the process of charge transfer is faster between electrode/electrolyte interface. The intersection of the semicircle at the high-frequency region of the Nyquist plot was further studied to obtain equivalence series resistance (ESR) values of the composites [21]. ESR is defined as the combination of resistance of solution, resistance within the electrode material, and resistance between the electrode material and current collectors [27]. It was found that the ESR value of PEDOT/GO/MnO$_2$ (45.8 Ω) is higher than PEDOT/GO (43.4 Ω) due to the nature of MnO$_2$ which suffers from low conductivity. At the low-frequency region of the Nyquist plots, both PEDOT/GO/MnO$_2$ and PEDOT/GO show a nearly vertical line, implying ideal capacitive behavior [8] and low diffusion resistance between the electrode materials and electrolyte ions [28]. The equivalent circuit of PEDOT/GO/MnO$_2$ and PEDOT/GO (Figure 7b) was developed using NOVA software by fitting the EIS data. Both equivalent circuits consist of ESR, R_{ct} parallel with double layer capacitance (C_{dl}), Warburg and constant phase element (CPE). CPE is added in order to take into account the inhomogeneity of the electrode after being modified. The chi-squares which represent the suitability of the equivalent circuit with the Nyquist plot of PEDOT/GO/MnO$_2$ and PEDOT/GO are 1.8×10^{-2} and 5.5×10^{-3} respectively. The low chi-square implies the better suitability of the equivalent circuit with the Nyquist plot.
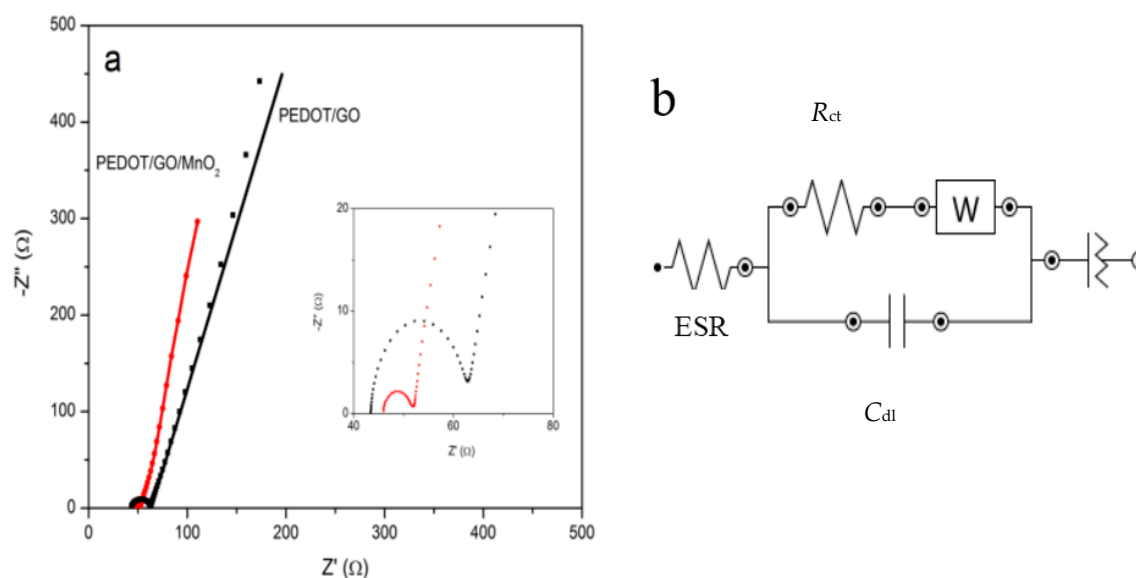
Figure 7. (**a**) Nyquist plot (inset shows magnified Nyquist plot) and (**b**) equivalent circuit of PEDOT/GO/MnO$_2$ and PEDOT/GO.

The stability of PEDOT/GO/MnO$_2$ (Figure 8) was measured using cyclic voltammetry and compared with PEDOT/GO for 1000 cycles at a scan rate of 100 mV/s. As shown in Figure 8, PEDOT/GO/MnO$_2$ is able to retain 95% of its original capacitance whereas PEDOT/GO only retains

79% after 1000 cycles. The synergistic effect contributed by each material plays an important role for better cycling stability. PEDOT is known for its low cycling stability due to swelling and shrinking of the polymer backbone [10] during cycling that leads to degradation of the conducting polymer [29]. GO which is known for its mechanical strength helps in contributing to the stability of the ternary composites [30]. The improvement of capacitance retention after 300 cycles of PEDOT/GO/MnO$_2$ could be attributed to complete wetting of the electrode materials by the electrolyte [29,31].
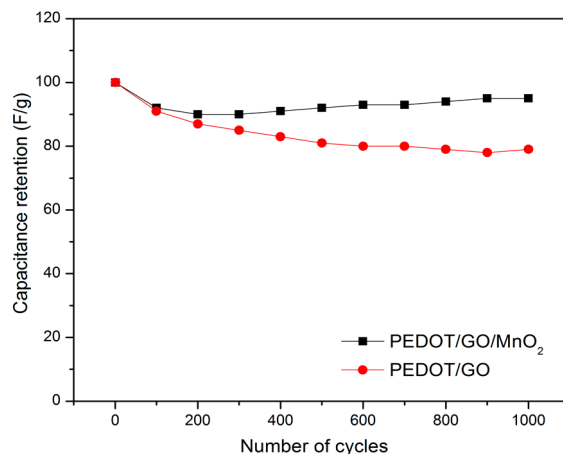

Figure 8. Stability test of PEDOT/GO/MnO$_2$ and PEDOT/GO.

3. Materials and Methods

3.1. Chemicals and Reagents

Manganese (II) sulphate monohydrate (MnSO$_4$·H$_2$O) and 3,4-ethylenedioxythiophene (EDOT) were purchased from Sigma-Aldrich, respectively. Ethanol was received from HmbG whereas acetone was acquired from Systerm. Potassium chloride (KCl) was purchased from Fisher Scientific and graphene oxide was attained from Graphenea. Deionized (DI) water was used throughout the experiments (18.2 MΩ·cm at 25 °C).

3.2. Preparation of PEDOT/GO/MnO$_2$ Composite

PEDOT/GO/MnO$_2$ was prepared via one step electrodeposition in a one compartment three-electrode configuration cell. Indium tin oxide (ITO, 1 cm^2) was used as a substrate and acted as a working electrode. Silver/silver chloride (Ag/AgCl) and platinum (Pt) coiled wire were employed as the reference and counter electrodes, respectively. The electrodepositions were performed using an Autolab M101 inside a Faraday cage at room temperature. The electrodeposition solution consists of 10 mM EDOT, 1.0 mg/mL GO and 0.025–0.3 M MnSO$_4$·H$_2$O. The electrodeposition was carried out at a constant potential of 1.2 V for 10 min.

3.3. Assembly and Characterization of Symmetric Electrodes

The symmetric supercapacitors were sandwiched together and separated by a filter paper soaked in 1 M KCl. The symmetric supercapacitors were then characterized by cyclic voltammetry (CV) in a potential range from 0 to 1 V, galvanostatic charge-discharge (GCD) and electrochemical impedance spectroscopy (EIS) at an amplitude of 5 mV with a frequency range between 0.1 Hz and 100 kHz at an open circuit potential (OCP). The surface morphology of the composites was studied by field emission scanning electron microscopy (FESEM, JEOL JSM-7600F, JEOL, ND, USA). The composition and structural analysis of the composites were analyzed using a Shimadzu XRD 6000 Diffractometer with Cu-K$_\alpha$ radiation (λ = 1.54 Å), a Raman spectrometer (WITec GmbH, Ulm, Germany), and an

X-ray photoelectron spectrometer (XPS XSAM HS Kratos Analytical). The binding energy of the XPS spectra was calibrated using the C 1s peak at 284.5 eV.

4. Conclusions

One-step electrodeposition has been successfully employed to fabricate $PEDOT/GO/MnO_2$ ternary composite. The ternary composite exhibits higher specific capacitance and better cycling stability performance, even after 1000 consecutive cycles, in comparison to the binary composite (PEDOT/GO). The high conductivity of PEDOT, the high surface area of GO, and the high specific capacitance of MnO_2 contribute to the supercapacitive performance of the ternary composite. MnO_2 also play a big role in maximizing the interaction of electrolyte ions and the electrode material by acting as a spacer in order to enhance the surface area of the ternary composite. Thus, $PEDOT/GO/MnO_2$ is a promising electrode material for a high-performance supercapacitor.

Author Contributions: N.H.N.A. performed the experiments. N.H.N.A. and Y.S. analyzed the data and wrote the paper. Y.S., L.H.N. and M.S.M. provided helpful discussion of the experimental design and data analysis.

Conflicts of Interest: The authors declare no conflict of interest.

References

1. Wang, G.; Zhang, L.; Zhang, J. A review of electrode materials for electrochemical supercapacitors. *Chem. Soc. Rev.* **2012**, *41*, 797–828. [CrossRef] [PubMed]
2. Raut, S.S.; Sankapal, B.R. Comparative studies on MWCNTs, Fe_2O_3 and Fe_2O_3/MWCNTs thin films towards supercapacitor application. *New J. Chem.* **2016**, *40*, 2619–2627. [CrossRef]
3. Chang, J.K.; Lee, M.T.; Huang, C.H.; Tsai, W.T. Physicochemical properties and electrochemical behavior of binary manganese-cobalt oxide electrodes for supercapacitor applications. *Mater. Chem. Phys.* **2008**, *108*, 124–131. [CrossRef]
4. Wang, Y.; Guo, J.; Wang, T.; Shao, J.; Wang, D.; Yang, Y.-W. Mesoporous transition metal oxides for supercapacitors. *Nanomaterials* **2015**, *5*, 1667–1689. [CrossRef] [PubMed]
5. Zhang, K.; Xu, J.; Zhu, X.; Lu, L.; Duan, X.; Hu, D.; Dong, L.; Sun, H.; Gao, Y.; Wu, Y. Poly(3,4-ethylenedioxythiophene) nanorods grown on graphene oxide sheets as electrochemical sensing platform for rutin. *J. Electroanal. Chem.* **2015**, *739*, 66–72. [CrossRef]
6. Cha, I.; Ji, E.; Seok, H.; Kim, J.-H.; Ho, Y.; Song, C. Facile electrochemical synthesis of polydopamine-incorporated graphene oxide/PEDOT hybrid thin films for pseudocapacitive behaviors. *Synth. Met.* **2014**, *195*, 162–166. [CrossRef]
7. Soojeong, L.; Suk Cho, M.; Hyuck, L.; Jae-Do, N.; Youngkwan, L. A facile synthetic route for well defined multilayer films of graphene and PEDOT via an electrochemical method. *J. Mater. Chem.* **2012**, *22*, 1899–1903.
8. Tang, P.; Han, L.; Zhang, L. Facile Synthesis of Graphite/PEDOT/MnO2 Composites on Commercial Supercapacitor Separator Membranes as Flexible and High-Performance Supercapacitor Electrodes. *ACS Appl. Mater. Interfaces* **2014**, *6*, 10506–10515. [CrossRef] [PubMed]
9. Yan, D.; Liu, Y.; Li, Y.; Zhuo, R.; Wu, Z.; Ren, P.; Li, S.; Wang, J.; Yan, P.; Geng, Z. Synthesis and electrochemical properties of MnO_2/rGO/PEDOT:PSS ternary composite electrode material for supercapacitors. *Mater. Lett.* **2014**, *127*, 53–55. [CrossRef]
10. Si, P.; Ding, S.; Lou, X.-W.; Kim, D.-H. An electrochemically formed three-dimensional structure of polypyrrole/graphene nanoplatelets for high-performance supercapacitors. *RSC Adv.* **2011**, *1*, 1271–1278. [CrossRef]
11. Mcallister, M.J.; Li, J.-L.; Adamson, D.H.; Schniepp, H.C.; Abdala, A.A.; Liu, J.; Herrera-alonso, O.M.; Milius, D.L.; Car, R.; Prud, R.K.; et al. Single sheet functionalized graphene by oxidation and thermal expansion of graphite. *J. Am. Chem. Soc.* **2007**, *19*, 4396–4404. [CrossRef]
12. Nabilah Azman, N.H.; Lim, H.N.; Sulaiman, Y. Effect of electropolymerization potential on the preparation of PEDOT/graphene oxide hybrid material for supercapacitor application. *Electrochim. Acta* **2016**, *188*, 785–792. [CrossRef]

13. Eeu, Y.C.; Lim, H.N.; Lim, Y.S.; Zakarya, S.A.; Huang, N.M. Electrodeposition of polypyrrole/reduced graphene oxide/iron oxide nanocomposite as supercapacitor electrode material. *J. Nanomater.* **2013**, *2013*, 1–6. [CrossRef]

14. Yu, D.; Yao, J.; Qiu, L.; Wang, Y.; Zhang, X.; Feng, Y.; Wang, H. In situ growth of Co_3O_4 nanoparticles on a-MnO_2 nanotubes: A new hybrid for high-performance supercapacitors. *J. Mater. Chem. A* **2014**, *2*, 8465–8471. [CrossRef]

15. Ye, Z.; Wang, B.; Liu, G.; Dong, Y.; Cui, X.; Peng, X.; Zou, A.; Li, D. Micropore-dominant Vanadium and Iron Co-doped MnO_2 hybrid film electrodes for high-performance supercapacitors. *J. Electrochem. Soc.* **2016**, *163*, A2725–A2732. [CrossRef]

16. Wei, C.; Pang, H.; Zhang, B.; Lu, Q.; Liang, S.; Gao, F. Two-Dimensional β-MnO_2 Nanowire Network with Enhanced Electrochemical Capacitance. *Sci. Rep.* **2013**, *3*, 2193. [CrossRef] [PubMed]

17. Wang, W.; Lei, W.; Yao, T.; Xia, X.; Huang, W.; Hao, Q.; Wang, X. One-pot synthesis of graphene/SnO_2/ PEDOT ternary electrode material for supercapacitors. *Electrochim. Acta* **2013**, *108*, 118–126. [CrossRef]

18. González, A.; Goikolea, E.; Barrena, J.A.; Mysyk, R. Review on supercapacitors: Technologies and materials. *Renew. Sustain. Energy Rev.* **2016**, *58*, 1189–1206. [CrossRef]

19. Lim, Y.S.; Tan, Y.P.; Lim, H.N.; Huang, N.M.; Tan, W.T.; Yarmo, M.A.; Yin, C.-Y. Potentiostatically deposited polypyrrole/graphene decorated nano-manganese oxide ternary film for supercapacitors. *Ceram. Int.* **2014**, *40*, 3855–3864. [CrossRef]

20. Wei, W.; Cui, X.; Chen, W.; Ivey, D.G. Manganese oxide-based materials as electrochemical supercapacitor electrodes. *Chem. Soc. Rev.* **2011**, *40*, 1697–1721. [CrossRef] [PubMed]

21. Sankar, K.V.; Selvan, R.K. The ternary $MnFe_2O_4$/graphene/polyaniline hybrid composite as negative electrode for supercapacitors. *J. Power Sources* **2015**, *275*, 399–407. [CrossRef]

22. Choi, H.-J.; Jung, S.-M.; Seo, J.-M.; Chang, D.W.; Dai, L.; Baek, J.-B. Graphene for energy conversion and storage in fuel cells and supercapacitors. *Nano Energy* **2012**, *1*, 534–551. [CrossRef]

23. Wu, Q.; Chen, M.; Wang, S.; Zhang, X.; Huan, L.; Diao, G. Preparation of sandwich-like ternary hierarchical nanosheets manganese dioxide/polyaniline/reduced graphene oxide as electrode material for supercapacitor. *Chem. Eng. J.* **2016**, *304*, 29–38. [CrossRef]

24. Pan, C.; Gu, H.; Dong, L. Synthesis and electrochemical performance of polyaniline @MnO_2/graphene ternary composites for electrochemical supercapacitors. *J. Power Sources* **2016**, *303*, 175–181. [CrossRef]

25. Han, G.; Liu, Y.; Kan, E.; Tang, J.; Zhang, L.; Wang, H.; Tang, W. Sandwich-structured MnO_2/polypyrrole/ reduced graphene oxide hybrid composites for high-performance supercapacitors. *RSC Adv.* **2014**, *4*, 9898–9904. [CrossRef]

26. Ramli, N.I.T.; Abdul Rashid, S.; Sulaiman, Y.; Mamat, M.S.; Mohd Zobir, S.A.; Krishnan, S. Physicochemical and electrochemical properties of carbon nanotube/graphite nanofiber hybrid nanocomposites for supercapacitor. *J. Power Sources* **2016**, *328*, 195–202. [CrossRef]

27. Zhou, H.; Zhai, H.-J.; Han, G. Superior performance of highly flexible solid-state supercapacitor based on the ternary composites of graphene oxide supported poly(3,4-ethylenedioxythiophene)-carbon nanotubes. *J. Power Sources* **2016**, *323*, 125–133. [CrossRef]

28. Shabani Shayeh, J.; Ehsani, A.; Ganjali, M.R.; Norouzi, P.; Jaleh, B. Conductive polymer/reduced graphene oxide/Au nano particles as efficient composite materials in electrochemical supercapacitors. *Appl. Surf. Sci.* **2015**, *353*, 594–599. [CrossRef]

29. Zhou, H.; Han, G.; Xiao, Y.; Chang, Y.; Zhai, H.-J. Facile preparation of polypyrrole/graphene oxide nanocomposites with large areal capacitance using electrochemical codeposition for supercapacitors. *J. Power Sources* **2014**, *263*, 259–267. [CrossRef]

30. Wang, W.; Hao, Q.; Lei, W.; Xia, X.; Wang, X. Graphene/SnO_2/polypyrrole ternary nanocomposites as supercapacitor electrode materials. *RSC Adv.* **2012**, *2*, 10268–10274. [CrossRef]

31. Prasankumar, T.; Irthaza Aazem, V.S.; Raghavan, P.; Prem Ananth, K.; Biradar, S.; Ilangovan, R.; Jose, S. Microwave assisted synthesis of 3D network of Mn/Zn bimetallic oxide-high performance electrodes for supercapacitors. *J. Alloys Compd.* **2017**, *695*, 2835–2843. [CrossRef]